A LETTERS JOURNAL EXPLORING THE FRONTIERS OF PHYSICS

Electric-field control of a magnetic phase transition in $Ni_3V_2O_8$

To cite this article: P. Kharel *et al* 2009 *EPL* **86** 17007

A Letters Journal Exploring the Frontiers of Physics

April 2009

EPL, **86** (2009) 17007
doi: 10.1209/0295-5075/86/17007

www.epljournal.org

Electric-field control of a magnetic phase transition in $Ni_3V_2O_8$

P. Kharel[1], C. Sudakar[1], A. Dixit[1], A. B. Harris[2], R. Naik[1] and G. Lawes[1(a)]

[1] *Department of Physics and Astronomy, Wayne State University - Detroit, MI 48201, USA*
[2] *Department of Physics, University of Pennsylvania - Philadelphia, PA 19104, USA*

received 5 February 2009; accepted in final form 17 March 2009
published online 22 April 2009

PACS 75.70.Ak – Magnetic properties of monolayers and thin films
PACS 77.80.Bh – Phase transitions and Curie point
PACS 75.30.Kz – Magnetic phase boundaries (including magnetic transitions, metamagnetism, etc.)

Abstract – We report on the electric-field tuning of a magnetic phase transition temperature (T_L) in multiferroic $Ni_3V_2O_8$ thin films. The simultaneous magnetic and ferroelectric transition in $Ni_3V_2O_8$ exhibits a clear dielectric anomaly; we monitored T_L under applied electric and magnetic fields using dielectric measurements. The transition temperature increases by $0.2\,K \pm 0.05\,K$ when the sample is biased approximately 25 MV/m compared to zero bias. This electric-field control of the magnetic transition can be qualitatively understood using a mean-field model incorporating a tri-linear coupling between the magnetic order parameters and spontaneous polarization. The shape of the electric field-temperature phase boundary is consistent with the proper order parameter for the multiferroic phase in $Ni_3V_2O_8$ being a linear combination of the magnetic and ferroelectric correlation functions.

Ferroelectric order and magnetic order are typically promoted by mutually exclusive properties. However, in certain special classes of materials long-range magnetic and ferroelectric order can develop concomitantly, with substantial coupling between the two [1]. In a number of these magnetoelectric multiferroics such as $TbMnO_3$ [2,3], $TbMn_2O_5$ [4], and $Ni_3V_2O_8$ [5,6] ferroelectric polarization can be controlled by an external magnetic field. Several models have been proposed for these multiferoics, including a Landau symmetry analysis for $Ni_3V_2O_8$ and similar systems [5,7–9], and a theory of ferroelectricity in inhomogeneous magnets based on a Ginzburg-Landau symmetry analysis [10].

There is considerable interest in understanding how an electric field can be used to control a magnetic structure, in part because of the possibility of developing novel devices based on voltage switchable magnetic memory [11]. It has been demonstrated that the magnetic structure can be modified electrostatically in certain multiferroic materials as demonstrated by optical studies on $HoMnO_3$ [12], photoemission electron microscopy in $BiFeO_3$ [13] and neutron scattering measurements in $TbMnO_3$ [14]. Recent studies have shown that the net magnetization can be switched using an applied electric field in $La_{0.67}Sr_{0.33}MnO_3/BaTiO_3$ epitaxial heterostructures [15], and controlled in a $BiFeO_3$-$CoFe_2O_4$ composite [16].

$Ni_3V_2O_8$ is a widely studied multiferroic material [5,17–21]. It is a magnetic insulator consisting of planes of spin-1 Ni^{2+} ions arranged in a kagome staircase lattice. $Ni_3V_2O_8$ undergoes a series of magnetic phase transitions at zero magnetic field. At $T_H = 9.1\,K$ it undergoes a magnetic transition into a high-temperature incommensurate (HTI) phase, described by the complex-valued order parameter σ_{HTI}. At $T_L = 6.3\,K$ $Ni_3V_2O_8$ undergoes a second phase transition into the low-temperature incommensurate (LTI) phase governed by a second complex order parameter σ_{LTI}. At lower temperatures, $Ni_3V_2O_8$ undergoes two additional phase transitions [5]. Most significantly for this work, $Ni_3V_2O_8$ also exhibits ferroelectric order in the LTI phase with a spontaneous polarization along the b-axis, which leads to a pronounced dielectric anomaly at the magnetic transition temperature T_L. $Ni_3V_2O_8$ is highly insulating and thin films can be easily prepared on a variety of substrates [22]. Theoretical predictions suggest that the ferroelectric LTI phase in $Ni_3V_2O_8$ should be stabilized in an electric field applied along the b-axis [23], with T_L being increased.

We have prepared thin films of $Ni_3V_2O_8$ by RF sputter deposition using a dense polycrystalline target prepared by standard solid-state techniques. Films with thickness

(a) E-mail: glawes@wayne.edu

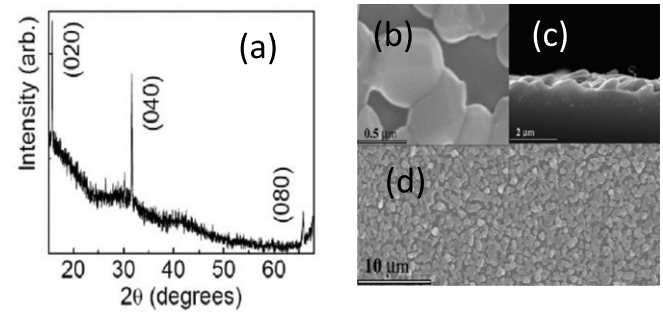

Fig. 1: a) XRD pattern for the $Ni_3V_2O_8$ thin film, b) SEM image (the scale bar is 500 nm), c) cross-section SEM image (the scale bar is 2 μm), d) SEM image (the scale bar is 10 μm).

from 500 nm to 600 nm were deposited on *a*-cut As-doped conducting silicon at 300 K; a more detailed discussion of thin film $Ni_3V_2O_8$ preparation is presented elsewhere [22]. These films were annealed in air for two hours at 1000 °C, which led to more highly oriented samples although the films exhibited a number of small pinhole defects. This led to frequent shorting when large top electrodes, having areas of ~ 20 to 30 mm^2, were deposited on the films. In order to mitigate the problems associated with pinhole defects, we deposited smaller gold contacts of only ~ 1 to 2 mm^2 directly on the smooth regions of thin films to serve as the top electrode. We investigated the crystal structure of the sputtered films using powder X-Ray Diffraction (XRD) on a Rigaku RU2000 diffractometer and film surfaces were imaged using the Scanning Electron Microscopy (SEM). We conducted dielectric and pyrocurrent measurements using an Agilent 4284A LCR meter and a Keithley 6517A electrometer, respectively, in conjunction to the PPMS.

X-ray diffraction patterns were collected at room temperature with copper K_α radiation in θ-2θ mode. The XRD pattern of the as-prepared films (not shown) showed only a diffused background, consistent with an amorphous sample. The diffraction peaks for the annealed samples, shown in fig. 1a, can be completely indexed to the $Ni_3V_2O_8$ structure (ref. PDF card No. 70-1394), with no impurity phases observed. Although the films are polycrystalline, the presence of only the (020), (040) and (080) peaks suggests that they are highly *b*-axis oriented. The SEM micrographs (figs. 1b–d) show that the films consist of faceted grains of approximately 1 μm to 2 μm diameter (figs. 1b and c). We estimate the thickness of the samples to be between 500 nm to 600 nm using the cross-sectional SEM micrograph (fig. 1c).

To probe the electric-field control of the LTI magnetic phase, we conducted dielectric measurements at $f = 30$ kHz at the LTI to HTI phase boundary while applying external electric and magnetic fields. There is no significant magnetic anomaly associated with the HTI to LTI magnetic phase boundary, but the dielectric constant is sharply peaked at this transition [24].

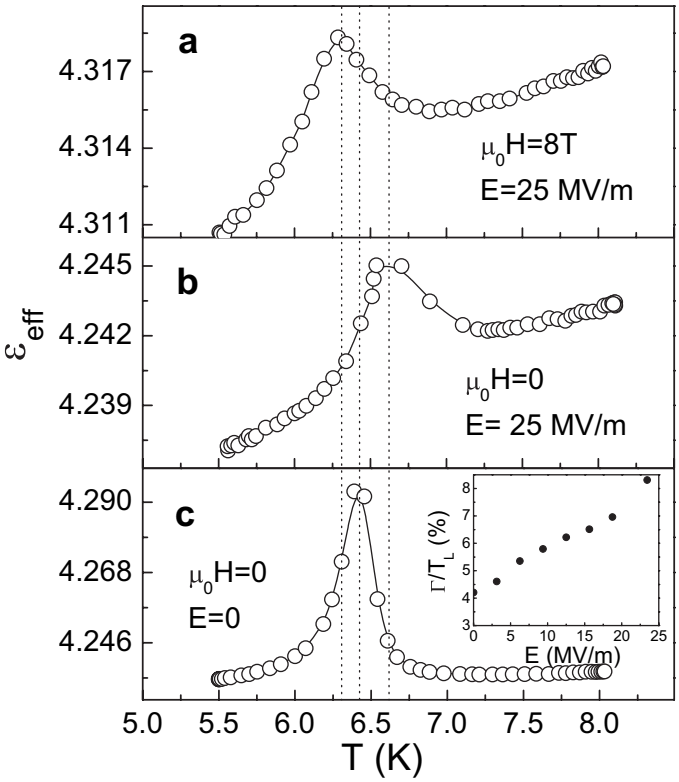

Fig. 2: Dielectric constant of the $Ni_3V_2O_8$ thin film measured at different electric and magnetic fields: a) $E = 25$ MV/m, $\mu_0 H = 8$ T, b) $E = 25$ MV/m, $H = 0$, c) $E = 0$, $H = 0$. The vertical dashed lines show transition temperatures for the different electric and magnetic fields. Inset: full-width half maximum (Γ) of the peak in dielectric constant, scaled to the transition temperature T_L, plotted against the applied electric field.

We plot the effective $Ni_3V_2O_8$ dielectric constant as a function of temperature under different representative external magnetic and electric fields in fig. 2. For these measurements, both the magnetic field and electric field are applied in the perpendicular direction, which is predominantly along the *b*-axis. With no external fields applied (fig. 2c), the dielectric constant shows a clear peak at $T_L = 6.3$ K. There is no clear sign of any dielectric feature associated with the LTI-CAF transition close to $T_C = 4$ K. This is consistent with dielectric measurements on the bulk polycrystalline $Ni_3V_2O_8$ (not shown), which are featureless at T_C, but unlike bulk single crystals, which show a large drop in ε at T_C [24]. When an average *b*-axis component of electric field $E = 25$ MV/m is applied to the sample (fig. 2b), this peak shifts up in temperature by approximately $\Delta T_L = 0.2\,\mathrm{K} \pm 0.05\,\mathrm{K}$, with the estimate of the error coming from the increase in the peak width. At still higher bias voltages, the data become increasingly noisy (not shown), which may indicate the onset of dielectric breakdown. We have observed this behavior in several samples indicating that the phenomenon is highly reproducible. The magnitude of the effective dielectric constant (approximately 4) is lower than that observed

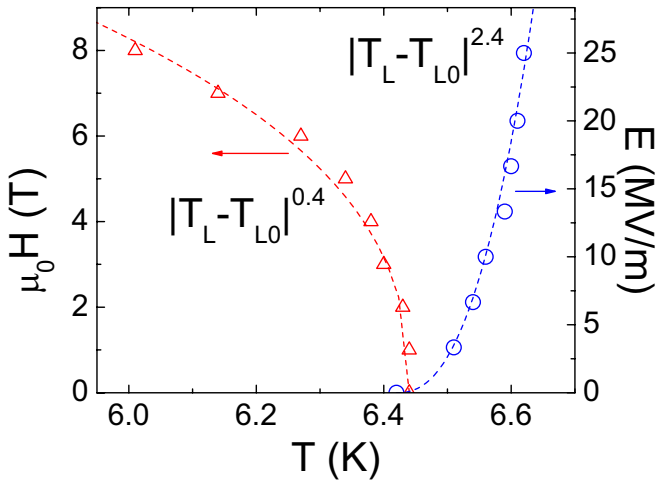

Fig. 3: (Colour on-line) E-H-T phase diagram near the HTI to LTI phase transition. The triangles show T_L measured as a function of magnetic field in zero electric field, while the circles show T_L measured as a function of electric field at zero magnetic field. The dashed lines are guides to the eye discussed in the text.

in single-crystal samples (approximately 6). We attribute this reduction to the fact that the $Ni_3V_2O_8$ film does not consist of a uniform coating of grains (see figs. 1b and d). This reduction in the volume fraction of $Ni_3V_2O_8$ in the films may lower the effective dielectric constant of the sample.

In order to eliminate the possibility that the magnetic and ferroelectric phase transitions split in finite electric fields, we also measured the $Ni_3V_2O_8$ dielectric constant under the simultaneous application of an electric field and magnetic field $\mu_0 H = 7.5\,T$ (fig. 2a). The single peak indicating the development of the LTI magnetic structure shifts down in temperature, confirming that this single multiferroic transition is sensitive to both magnetic and electric fields. There is, however, considerable broadening observed in the dielectric anomaly with increasing electric field. This is shown in the inset of fig. 2c, which plots the full-width half maximum (Γ) of the peak in dielectric constant relative to the transition temperature T_L against the applied electric field. The monotonic broadening of the dielectric response with increasing electric field is similar to the broadening observed in ferromagnetic transitions in an external magnetic field [25]. This is consistent with the suggestion that the development of the multiferroic state in $Ni_3V_2O_8$ in a finite electric field is a cross-over phenomena rather than a proper thermodynamic phase transition [11].

We summarize the results of our measurements on the electric- and magnetic-field dependence of the HTI to LTI magnetic phase transition in fig. 3. The dashed lines are guides to the eye for the phase boundaries and are discussed in the following. The circles in fig. 3 show the bias voltage *vs.* the LTI transition temperature at $H = 0\,\mathrm{Oe}$, determined by dielectric measurements similar to those plotted in fig. 2. We find that applying an electric field parallel to the b-axis in $Ni_3V_2O_8$ stabilizes the ferroelectric LTI magnetic structure, as predicted theoretically. We also confirm that an external magnetic field shifts the T_L transition temperature, as shown by the triangles in fig. 3. This shift is comparable to what has been observed in bulk $Ni_3V_2O_8$ samples [5], although this very small shift is difficult to resolve when the phase diagram is plotted over the entire temperature range. The phase boundaries can be approximately fit to power law behaviour. The magnetic field-temperature (H-T) phase boundary has a functional form given by $H \sim |T_L - T_{L0}|^{0.4}$, with T_L the transition temperature at a magnetic field H and T_{L0} the zero-field transition temperature. This is consistent with predictions [19] that the HTI-LTI phase boundary should scale with magnetic field as $T_L(H) \sim T_{L0} - AH^2$, with T_{L0} the zero-field transition temperature, as H is a non-critical field for the LTI order parameter. This expression would predict an exponent of 0.5 rather than the 0.4 observed experimentally, but the discrepancy is well within the experimental uncertainty. We also observe a shift in the multiferroic transition temperature T_L with applied electric field, with the electric field-temperature (E-T) phase boundary having a functional form given by $E \sim (T - T_L)^{2.4}$. While the absolute magnitude of the shift in T_L with electric field is small, reaching only 0.2 K in an applied field of 25 MV/m, the size of this change is roughly consistent with predictions for changes in the LTI to CAF transition temperature in finite fields, and can be attributed to the very small ferroelectric polarization in $Ni_3V_2O_8$ [11].

This dependence of the E-T phase boundary can be understood qualitatively within the framework of a mean-field trilinear coupling between the LTI and HTI magnetic-order parameters and the spontaneous polarization [11]. This model predicts the onset of ferroelectric order associated with the magnetic structure in the LTI phase of $Ni_3V_2O_8$, but also predicts that inducing a polarization by applying an external electric field should stabilize the LTI magnetic structure [11]. These experimental studies also provide some guidance on identifying the proper multiferroic order parameter for $Ni_3V_2O_8$. In the framework of this mean-field model, we suppose that the applied electric field along the b-axis produces an electric polarization (P_b), which in turn couples to the LTI phase magnetic order parameter (σ_{LTI}). To see this in more detail we write the free energy near the LTI-HTI phase boundary as

$$\begin{aligned} F \;=\; & \tfrac{1}{2}\chi_{\mathrm{E}}^{-1} P^2 + ia\left(\langle\sigma^*_{\mathrm{HTI}}\rangle\sigma_{\mathrm{LTI}} - \langle\sigma_{\mathrm{HTI}}\rangle\sigma^*_{\mathrm{LTI}}\right) P_b \\ & + \tfrac{1}{2}\left(T - T_{\mathrm{L}}\right)\left|\sigma_{\mathrm{LTI}}\right|^2 - \vec{E}\cdot\vec{P}, \end{aligned} \tag{1}$$

where χ_{E} is the electric susceptibility, and a is a constant. Since the LTI-HTI phase boundary is far from the transition to the HTI phase, we replace the HTI magnetic order parameter, σ_{HTI}, by its average value $\langle\sigma_{\mathrm{HTI}}\rangle$. The true LTI order parameter, $\tilde{\sigma}$, is found by diagonalizing the

quadratic form in P_b and σ_{LTI}, and is therefore given by

$$\tilde{\sigma} = b\sigma_{\mathrm{LTI}} + b^* \sigma^*_{\mathrm{LTI}} + cP_b. \quad (2)$$

From this expression, one sees that an applied electric field acts as a field conjugate to the real order parameter $\tilde{\sigma}$. Because the coefficient a in eq. (1) is small, as evidenced by the very small spontaneous polarization in $Ni_3V_2O_8$, the contribution of P to the proper order parameter is also small. This is why we did not need to consider any effect of the polarization contribution to the order parameter to explain the shape of the H-T phase boundary. Near the LTI-HTI phase boundary the order parameter can be written as

$$\langle \tilde{\sigma} \rangle = t^{\beta} F\left(Et^{-\beta-\gamma}\right), \quad (3)$$

where F is an unknown scaling function and β and γ are the usual critical exponents for the magnetization and susceptibility respectively [26]. The LTI-HTI phase boundary occurs when the scaling variable $Et^{-\beta-\gamma}$ assumes a critical value and thus the phase boundary is given by $E \sim \Delta T^{\beta+\gamma}$. Within mean-field theory $\beta = 1/2$ and $\gamma = 1$, which would lead to $E \sim (\Delta T)^{1.5}$, but fluctuations lead to a significant increase in γ and usually a smaller decrease in β, so that typically one expects $\gamma + \beta \sim 1.7$. This is somewhat smaller than the exponent of 2.4 seen as the dashed line fit plotted in fig. 3, but this model provides at least a qualitative explanation for the shape of the E-T phase boundary curve. Because the real order parameter, $\tilde{\sigma}$, couples to an applied electric field, we believe that the symmetry of the HTI phase is broken by the external electric field, so that the HTI to LTI transition in finite E-fields is a cross-over effect rather than a real thermodynamic phase transition.

In conclusion, we have demonstrated that the temperature for a magnetic phase transition in $Ni_3V_2O_8$ thin films can be controlled using an external electric field. Because of the coupling between the magnetic and ferroelectric order parameters, the LTI phase is stabilized by the application of an electric field, as confirmed by dielectric measurements. This effect is complementary to the magnetic-field control of the ferroelectric transition temperature observed in many other multiferroic systems [2–5]. Furthermore, we find that the low field phase boundaries for the HTI-LTI phase transition in $Ni_3V_2O_8$ are consistent with the power law scaling one would expect for an order parameter consisting of both magnetic and ferroelectric components, both for a non-critical H-field shifting an antiferromagnetic transition and a critical E-field coupling to the polarization. While the E-field–induced shifts in this magnetic transition temperature were very small, we expect that higher-quality samples having better orientation may show stronger coupling. Furthermore, different multiferroic materials having larger values of ferroelectric polarization may be expected to show larger E-field–induced shifts in transition temperature, as the change of transition temperature in finite electric fields is expected to be proportional to the magnitude of the polarization [11]. The ability to switch the magnetization using a bias voltage is an important characteristic for many of the proposed potential applications for multiferroic materials.

* * *

This work was supported by the NSF under DMR-0644823, and by the Wayne State University Institute for Manufacturing Research.

REFERENCES

[1] Hill N. A., *J. Phys. Chem. B*, **104** (2000) 6694.
[2] Kimura T., Goto T., Shintani H., Ishizaka K., Arima T. and Tokura Y., *Nature*, **426** (2003) 55.
[3] Kimura T., Lawes G., Goto T., Tokura Y. and Ramirez A. P., *Phys. Rev. B*, **71** (2005) 224425.
[4] Hur N., Park S., Sharma P. A., Ahn J. S., Guha S. and Cheong S.-W., *Nature*, **429** (2004) 392.
[5] Lawes G., Harris A. B., Kimura T., Rogado N., Cava R. J., Aharony A., Entin-Wohlman O., Yildirim T., Kenzelmann M., Broholm C. and Ramirez A. P., *Phys. Rev. Lett.*, **95** (2005) 087205.
[6] Chaudhury R. P., Yen F., dela Cruz C. R., Lorenz B., Wang Y. Q., Sun Y. Y. and Chu C. W., *Phys. Rev. B*, **75** (2007) 012407.
[7] Harris A. B., *J. Appl. Phys.*, **99** (2006) 08E303.
[8] Kenzelmann M., Harris A. B., Jonas S., Broholm C., Schefer J., Kim S. B., Zhang C. L., Cheong S.-W., Vajk O. P. and Lynn J. W., *Phys. Rev. Lett.*, **95** (2005) 087206.
[9] Harris A. B., *Phys. Rev. B*, **76** (2007) 054447.
[10] Mostovoy M., *Phys. Rev. Lett.*, **96** (2006) 067601.
[11] Haris A. B. and Lawes G., *The Handbook of Magnetism and Advanced Magnetic Materials* (Wiley, London) 2007.
[12] Lottermoser T., Lonkai T., Amann U., Hohlwein D., Ihringer J. and Fiebig M., *Nature*, **430** (2004) 541.
[13] Zhao T., Scholl A., Zavaliche F., Lee K., Barry M., Doran A., Cruz M. P., Chu Y. H., Ederer C., Spaldin N. A., Das R. R., Kim D. M., Baek S. H., Eom C. B. and Ramesh R., *Nat. Mater.*, **5** (2006) 823.
[14] Yamasaki Y., Sagayama H., Goto T., Matsuura M., Hirota K., Arima T. and Tokura Y., *Phys. Rev. Lett.*, **98** (2007) 147204.
[15] Eerenstein W., Wiora M., Prieto J. L., Scott J. F. and Mathur N. D., *Nat. Mater.*, **6** (2007) 348.
[16] Zavaliche F., Zhao T., Zheng H., Straub F., Cruz M. P., Yang P.-L., Hao D. and Ramesh R., *Nano Lett.*, **7** (2007) 1586.
[17] Sauerbre E. E., Faggiani R. and Calvo C., *Acta Crystallogr. B*, **29** (1973) 2304.
[18] He Z., Ueda Y. and Itoh M., *J. Cryst. Growth*, **297** (2006) 1.
[19] Kenzelmann M., Harris A. B., Aharony A., Entin-Wohlman O., Yildirim T., Huang Q., Park S., Lawes G., Broholm C., Rogado N., Cava R. J., Kim K. H., Jorge G. and Ramirez A. P., *Phys. Rev. B*, **74** (2006) 014429.

[20] Rogado N., Lawes G., Huse D. A., Ramirez A. P. and Cava R. J., *Solid State Commun.*, **124** (2002) 229.
[21] Lawes G., Kenzelmann M., Rogado N., Kim K. H., Jorge G. A., Cava R. J., Aharony A., Entin-Wohlman O., Harris A. B., Yildirim T., Huang Q. Z., Park S., Broholm C. and Ramirez A. P., *Phys. Rev. Lett.*, **93** (2004) 247201.
[22] Sudakar C., Kharel P., Naik R. and Lawes G., *Philos. Mag. Lett.*, **87** (2007) 223.
[23] Harris A. B., Yildirim T., Aharony A. and Entin-Wohlman O., *Phys. Rev. B*, **73** (2006) 184433.
[24] Lawes G., Kimura T., Varma C. M., Subramanian M. A., Cava R. J. and Ramirez A. P., *The Twelfth US-Japan Seminar on Dielectric and Piezoelectric Ceramics*, (2005) p. 215, arXiv:0904.1974.
[25] Flax L., *Phys. Rev. B*, **5** (1972) 977.
[26] Stanley H. E., *Introduction to Phase Transitions and Critical Phenomena* (Oxford University Press) 1986.